Optimum Switching Scenario Analysis in a Dynamic Entanglement Network

R. Wang [1,*], M. J. Clark[2], S. K. Joshi[2], S. Bahrani[1], O. Alia[1], M. Peranić[3], M. Lončarić[3], M. Stipčević[3], J. Rarity[2], R. Nejabati[1], D. Simeonidou[1]

[1] *High Performance Networks Group, Merchant Venturers Building, University of Bristol, UK.*
[2] *Quantum Engineering Technology Labs, & H. H. Wills Physics Laboratory, University of Bristol, UK.*
[3] *Center of Excellence for Advanced Materials and Sensing Devices, Ruđer Bošković Institute, Zagreb, Croatia.*
[*] *rui.wang@bristol.ac.uk*

Abstract: We investigate the performance of a dynamical entanglement-based QKD network with various switching scenarios. The simulation results suggest the optimum scenario for different heralding efficiencies and detectors' jitter and the experimental results verify the benefit. © 2022 The Author(s)

1. Introduction

With recent advancements in quantum technologies, entanglement-based quantum networks utilising a broadband spontaneous parametric down-conversion (SPDC) can provide an efficient approach for distributing entangled photon pairs to many users. The implementation of entanglement-based quantum networks for 4 nodes has been first demonstrated in [1]. Later in [2], Dense wavelength-division multiplexing and beam-splitting techniques were adopted to expand to 8 users. Entanglement distribution with active switching using wavelength selective switch (WSS) was reported in [3, 4]. Recently, with the implementation of a quantum reconfigurable optical add-drop multiplexer (q-ROADM), a dynamic and scalable entanglement-based network has been developed [5] to offer on-demand entanglement distribution based on the requirements of applications.

Many applications e.g. multi-user entanglement-based quantum key distribution (QKD), don't need dedicated connectivity that is active all time if the link between two users has sufficient keys. Dynamical switching allows the redistribution of the limited entanglement resources to support other nodes. Furthermore, dynamical switching between different sub-mesh topologies can form a fully-connected graph with keys accumulated between any user pairs due to the nature of the QKD described above. One central question arising here is whether such dynamic switching would provide any benefit to network performance, e.g. increasing the overall secret key rate (SKR). In this paper, we extensively explore the effect of dynamic reconfiguration of entanglement-based QKD network interconnections with three partial-mesh switching scenarios and compare them with the full-mesh case. Various system parameters such as laser pump power, jitter of detectors and heralding efficiency (HE) of the entanglement source are considered and we explore the operation scenarios where the network's performance is optimum.

2. Evaluation Setup, Results and Discussion

The entanglement network setup is illustrated in Fig. 1A. The broadband entangled source (type-0 SPDC) produces state $\Phi^+ = \frac{1}{\sqrt{2}}(|H_sH_i\rangle + |V_sV_i\rangle)$. The q-ROADM consists of an optical fibre switch (OFS) interconnecting a spectrum-splitting DEMUX and multiple channel-combining MUX/WSS. It offers on-demand entanglement distribution to 6 users, namely Alice (A), Bob (B), Chloe (C), Dave (D), Faye (F) and Gopi (G). Each user employs two superconducting nanowire single-photon detectors (SNSPDs) and a polarisation analysis module (PAM). In PAM, photons randomly transmit or are reflected by the beam splitter (BS), in which the short path is defined as HV basis and the long path is defined as DA basis. PBS performs the polarisation measurement, the time tagger registers the time for each click of the detectors and users share the timestamp with each other to perform temporal cross-correlation. The entanglement source, user modules are deployed at NSQI, and q-ROADM is at HPN interconnected by field-deployed fibre between HPN and NSQI (1.6 km in total), apart from user D containing the metropolitan link (5.6 km) bouncing back at Watershed, as shown in Fig. 1B.

The experiment with source HE (∼16%) and jitter of SNSPDs (∼100 ps) shows the 6-user network can accumulate more keys through full-mesh (FM) setting compared to dynamically switching between two sub-scenarios in 2 partial-mesh (2PM) setting (see in Fig. 1C) for most quantum links, as shown in Fig. 2A. We simulate the performance of each link using the same network parameters for FM and 2PM scenarios. The coincidence window of each link is selected via a pre-calculated look-up table to maximise the SKR. The average SKR of each link is plotted in Fig. 2B. The performance of the majority of links from the simulation fits well with the experimental data. The gap is mainly due to different detectors' jitters/efficiency, the coupling efficiency of PAM, measurement precisions like source HE, link loss, and changes in the environment, such as temperature and vibration.

However, in our previous experiment (Fig.3a in [5]), 2PM could outperform FM with source HE $\sim$ 3% and detectors' jitter 200-300 ps. To understand the potential optimal scenario to operate with different source HEs and detectors' jitters, 4 scenarios are investigated presenting different levels of connectivities per user, namely

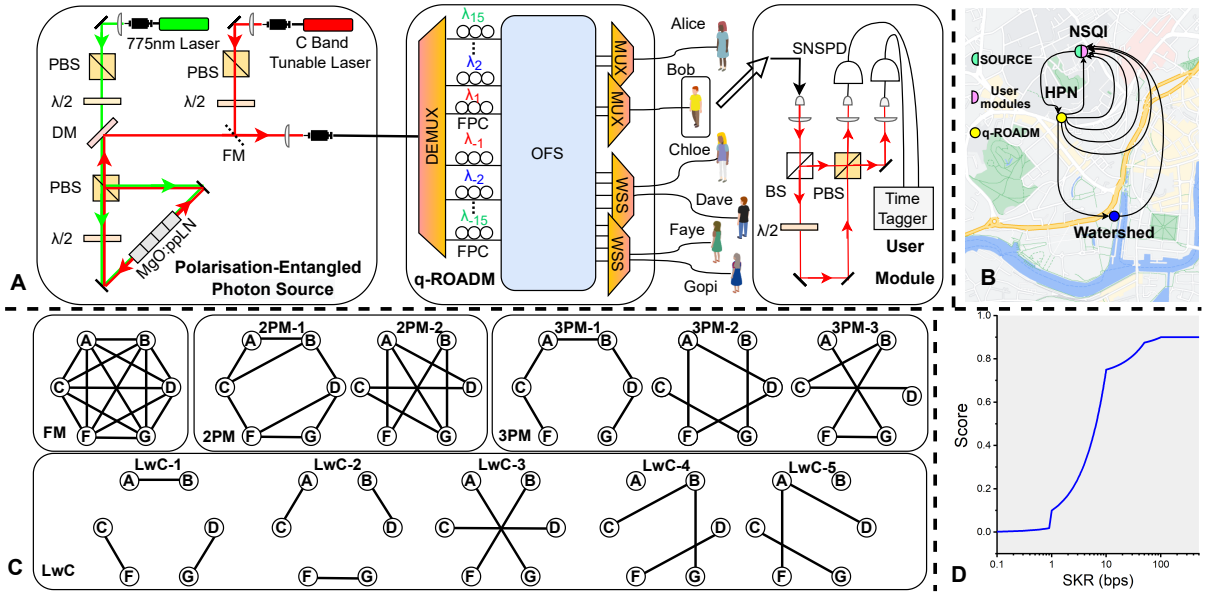

Fig. 1: Entanglement network setup, physical connectivities, reconfiguration scenarios and performance scoring function. (A): Diagram of the 6-user entanglement-distribution network; (B) 6 Users connected to the source via q-ROADM through the Bristol campus and metropolitan fibre links. (C) Four dynamic configuration scenarios: FM, 2PM, 3PM and LwC. (D) Scoring function to evaluate the performance of a QKD link.

FM, 2PM, 3 partial-mesh (3PM) and link-wise connectivities (LwC), as shown in Fig. 1C. With the FM setting, the network's configuration is fixed. The rest individual scenario requires switching between the sub-scenarios to form full-mesh connectivities in a time-shared manner. To evaluate the performance of different scenarios, we designed a scoring system (see in Fig. 1D) using the interpolation as a function of the average SKR of each link. For example, the average SKR of A-B link in LwC is the number of keys generated in the LwC-1 sub-scenario divided by the total time of executing sub-scenarios from LwC-1 to LwC-5. The overall network-wise score is calculated by multiplying the scores of all sub-scenarios while a sub-scenario score is given by its active links. The scenario with a higher score is defined to perform better than low-score scenarios. Based on the network-wise score, the average effective (AE)-SKR of the network is calculated as an inverse of the interpolation function: $f^{-1}(Score_{net}^{-l_n})$, where l_n is the total link number of all sub-scenarios and $l_n = 15$ in our case.

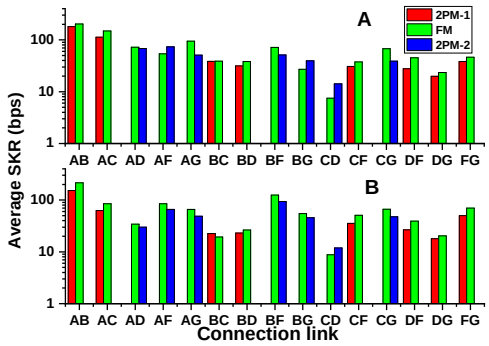

Fig. 2: Average SKR of FM and 2PM scheme (A) Experimental results. (B) Simulation results.

The source laser pump power can be adjusted to optimise the performance of each sub-scenario and the maximum singles rate is capped at 2 million per second per 100 GHz channel, matching the maximum brightness of the source from the experiment. The jitter of detectors of all the users are assumed to be identical varying from 50 ps to 500 ps and the source heralding efficiency is set between 1% and 20% to model different operational conditions. In Fig. 3, the optimal AE-SKR heatmap is plotted with different jitters and source HE for 4 scenarios. The FM starts to fail at 8.6% HE with 0 bps AE-SKR when compared to 2.9% for 2PM and 1% for 3PM and LwC when the jitter is 500 ps. Since each user in FM receives 5 channels simultaneously, the accidentals rate is higher compared to other scenarios. This leads to the quantum bit error rate (QBER) of some links being higher than the 11% threshold for QKD when HE is below 10.5%. In contrast, other scenarios with each user receiving fewer channels can work at 8.6% HE. In the low-jitter region with fewer accidentals, all the scenarios are successful in providing positive SKR. It is worth noting that FM outperforms LwC and 3PM in high HE and low jitter settings since FM, even with relatively lower SKR, is operating full time so can accumulate more keys than 3PM or LwC with high SKR but in a time-shared way.

The network-wise AE-SKR comparison between other scenarios and FM is illustrated in Fig. 4. The black cells mean the FM fails, while the white cells represent the performance of the two scenarios is equivalent. From the figure, 2PM performs better than FM under all conditions, whereas 3PM can achieve wider areas (in HE and jitters) of >1 dB AE-SKR improvement over FM compared to 2PM. For LwC vs FM, the AE-SKR of LwC is higher than FM apart from networks operating in low-jitter and high-HE regions, where FM can yield higher AE-SKR.

The maximum brightness of the entanglement source varies between platforms and hardware. The optimum scenario distribution against HE and jitters are depicted in Fig. 5 with the maximum singles rate per channel

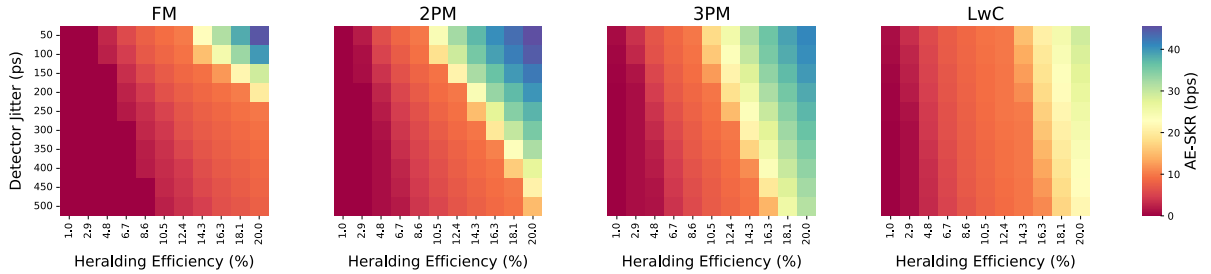

Fig. 3: Network-wise AE-SKR distribution with different HE and detectors' jitter for FM, 2PM, 3PM and LwC.

capped at 1E6, 2E6 and 5E6. The results indicate when the maximum singles rate is 5E6, the optimum scenario is selected between LwC and 3PM. Higher pump power leads to more coincidences for sub-scenarios in LwC and 3PM, but maintains QBER at a relatively low level due to 1-2 channels at each user. This results in a higher average SKR even requiring switching between sub-scenarios in time. When the maximum singles rate is capped at 1E6, LwC only shows advantages at low HE regions while 3PM is the optimum scenario in low-jitter low-HE and high-jitter high-HE regions. The simulation results with the max singles rate of 1E6 in Fig.5 also verify the experimental outcome in which FM performs better than 2PM with 16% HE and detectors' jitter of 100 ps as shown in Fig. 2A), while 2PM outperforms FM with ∼3% HE and jitter of 200-300 ps (see Fig.3a in [5]).

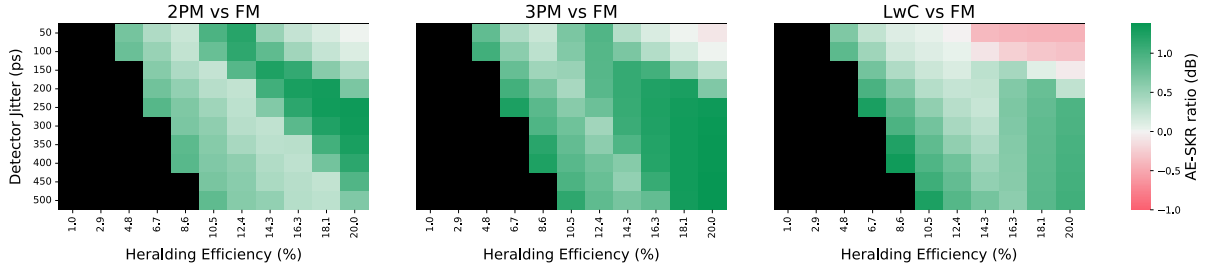

Fig. 4: Network-wise average effective-SKR comparison between FM and other scenarios.

In summary, we study the impact of several reconfiguration scenarios on the performance of the Bristol entanglement-based network via extensive simulation. The results suggest an optimum reconfiguration scenario with the network under different source heralding efficiencies, brightness, and detectors' jitter. The experimental results also verify the outcome of the simulation.

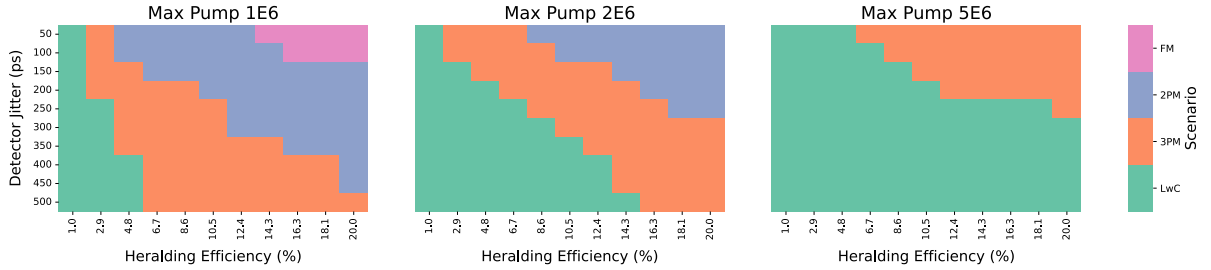

Fig. 5: Optimum scenario selection with different levels of maximum source brightness.

Acknowledgements

We acknowledge the funding support from the Quantum Communication Hub (EP/T001011/1), IUK Quantum Data Centre of the Future project, and from the Ministry of Science and Education (MSE) of Croatia (contract No. KK.01.1.1.01.0001)

References

1. S. Wengerowsky, S. K. Joshi, F. Steinlechner, H. Hübel, and R. Ursin, "An entanglement-based wavelength-multiplexed quantum communication network," *Nature*, vol. 564, no. 7735, pp. 225–228, 2018.
2. S. K. Joshi, D. Aktas, S. Wengerowsky, M. Lončarić, S. P. Neumann, B. Liu, T. Scheidl, G. C. Lorenzo, Ž. Samec, L. Kling *et al.*, "A trusted node–free eight-user metropolitan quantum communication network," *Science advances*, vol. 6, no. 36, p. eaba0959, 2020.
3. N. B. Lingaraju, H.-H. Lu, S. Seshadri, D. E. Leaird, A. M. Weiner, and J. M. Lukens, "Adaptive bandwidth management for entanglement distribution in quantum networks," *Optica*, vol. 8, no. 3, pp. 329–332, 2021.
4. F. Appas, F. Baboux, M. I. Amanti, A. Lemaítre, F. Boitier, E. Diamanti, and S. Ducci, "Flexible entanglement-distribution network with an algaas chip for secure communications," *npj Quantum Information*, vol. 7, no. 1, pp. 1–10, 2021.
5. R. Wang, O. Alia, M. Clark, S. Bahrani, S. K. Joshi, D. Aktas, G. T. Kanellos, M. Peranić, M. Lončarić, M. Stipčević *et al.*, "A dynamic multi-protocol entanglement distribution quantum network," in *2022 Optical Fiber Communications Conference and Exhibition (OFC)*. IEEE, 2022, pp. 1–3.